Layered Perovskites with Giant Spontaneous Polarizations for Nonvolatile Memories

Uong Chon,[1,2] Hyun M. Jang,[1,*] M. G. Kim,[3] and C. H. Chang[2]
[1]*Department of Materials Science and Engineering, and National Research Laboratory for Ferroelectric Phase Transitions, Pohang University of Science and Technology (POSTECH), Pohang 790-784, Republic of Korea*
[2]*Research Institute of Industrial Science and Technology (RIST), Pohang 790-330, Republic of Korea*
[3]*Pohang Accelerator Laboratory (PAL), Pohang University of Science and Technology (POSTECH), Pohang 790-784, Republic of Korea*

(Received 11 December 2001; published 5 August 2002)

A series of titanate-based layered perovskites having large values of the spontaneous polarization P_s were developed for their applcations to *nonvolatile ferroelectric random access memories*. Among these, the Nd-modified bismuth titanate [$Bi_{4-x}Nd_xTi_3O_{12}$ (BNdT)] system exhibited the most remarkable ferroelectric properties. The c-axis oriented BNdT capacitor was characterized by a switchable remanent polarization $2P_r$ of over 100 $\mu C/cm^2$ and imprinting and fatigue-free behavior. The active Ti site responsible for the giant P_s was identified with the help of Rietveld analysis, x-ray absorption near-edge structure study, and *ab initio* quantum computations.

DOI: 10.1103/PhysRevLett.89.087601 PACS numbers: 85.50.–n, 77.55.+f, 77.80.–e, 77.84.Dy

In modern technology involving ferroelectrics, the ever-increasing demands for nonvolatile memories [1–3] have led to the search for a new material having a large spontaneous polarization P_s with fatigue-resistant characteristics for high-density memories and for the reliability of performances. Among many materials that exhibit ferroelectricity, only two families of perovskites are currently scrutinized for their use in nonvolatile memories: (i) PZT(lead zirconate titanate)-based perovskites [2–6] and (ii) layered perovskites such as strontium bismuth tantalate (SBT) [7] and lanthanum-modified bismuth titanate (BLT) [8,9]. PZT-based perovskites have been studied extensively, but a poor fatigue resistance makes them inapplicable to direct commercialization using common Pt electrodes. The fatigue resistance can be significantly improved by employing metal-oxide electrodes including RuO_2 and Ir/IrO_2 [4,5]. However, they are electrically leaky, in general, and make the process more complicated. On the other hand, SBT and BLT show a superior fatigue resistance as compared to PZT/Pt. However, SBT suffers from some disadvantages, such as high-processing temperatures and very low switchable remanent polarization ($2P_r$) values.

As one of few fatigue-free ferroelectrics [8,9], BLT ($Bi_{4-x}La_xTi_3O_{12}$) is currently regarded as one of the most promising candidate materials [3] for *nonvolatile ferroelectric random access memories* (NvFRAM). However, the BLT film prepared by pulsed laser deposition (PLD) was characterized by a mixed orientation of grains [8]. The mixed orientation tends to increase bit-to-bit variability in a capacitor for high-density memory devices [3]. In addition to this, the sensing margin (i.e., $2P_r$ value) of the BLT capacitor is not satisfactory to be adopted in high-density memory devices that require reliability in their performances. Our preliminary study indicated that the direction and the magnitude of $2P_r$ of highly c-axis oriented bismuth titanate (BT)-based films were very susceptible to the substitution of trivalent rare-earth cations for bismuth [10]. Thus, one would expect to obtain BT-based thin films having both fatigue-free characteristics and large P_s by suitably substituting trivalent ions for volatile bismuth ions that tend to destabilize the oxygen ions located at the Ti-O octahedron layer [8]. Among many rare-earth (Re) cations, Pr, Nd, Sm, and Gd meet the requirements of the ionic radius, the stable Curie temperature ($> 400\,^\circ C$), and the phase stability of $(BiO)_2Re_2Ti_3O_{10}$-type layered perovskites [11]. In view of these, the main objective of the present study is to develop rare-earth-cations-modified titanate films suitable for the realization of high-density NvFRAM devices.

For this purpose, a series of rare-earth-cation-modified BT films were prepared, employing two distinctive methods: PLD and sol-gel coating. The PLD method tends to produce (001)-oriented films but with a mixed orientation of grains, including (117) orientation. Thus, we focus mainly on the sol-gel processed films hereafter. The precursor sol for the BNdT film, for example, was prepared by first dissolving appropriate amounts of bismuth acetate and neodymium acetate hydrate in an acidic solution at room temperature. 4-mol % excess bismuth acetate was used to compensate the Bi loss that was induced during the thermal annealing of amorphous films. A stoichiometric amount of titanium isopropoxide solution was slowly added to the mixed precursor solution [10]. The resulting sols were stable over a period of months. BT-based films with their thickness of 280 ± 10 nm were annealed in an oxygen-rich atmosphere at 650 °C for 1 h.

Figure 1 compares the polarization vs electric field (P-E) switching curve of the BNdT film ($Bi_{4-x}Nd_xTi_3O_{12}$ with $x = 0.85$) with that of the BT ($x = 0$) film grown on $Pt/TiO_2/SiO_2/Si(100)$ substrates. Both films are highly c-axis oriented [Fig. 1(b)] and have a homogeneous in-plane alignment of grains, as examined by their φ-scan spectra. Thus, the result presented in

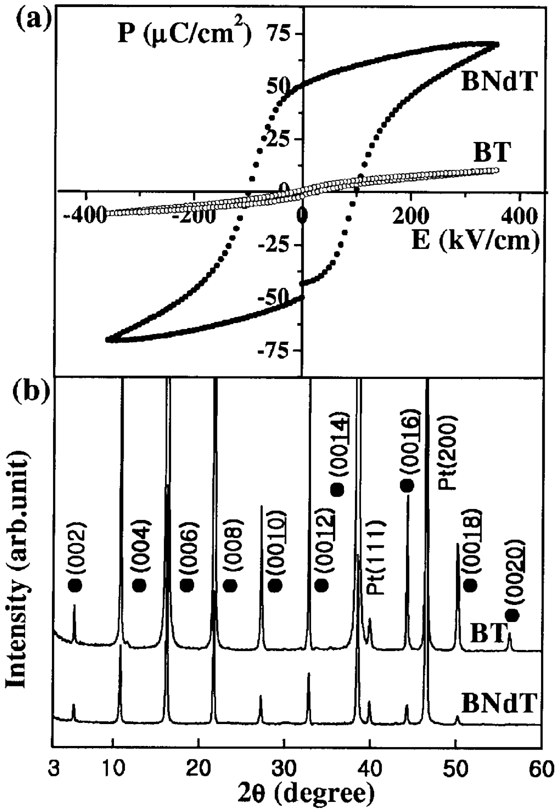

FIG. 1. *P-E* hysteresis loops and XRD patterns of bismuth titanate-based perovskites. (a) *P-E* hysteresis loops of *c*-axis oriented BT and BNdT film capacitors at an applied voltage of 10 V. (b) XRD patterns of BT and BNdT films on Pt/TiO_2/SiO_2/Si(100) substrates, showing a highly *c*-axis oriented preferential growth.

Fig. 1(a) demonstrates a noticeable increase in P_s (or $2P_r$) parallel to the c axis by the partial substitution of Nd for Bi. The giant polarization ($2P_r = 103\ \mu\mathrm{C/cm^2}$) observed in the Pt/BNdT/Pt capacitor is remarkable in a sense that $2P_r$ of the PLD grown BLT is only 24 $\mu\mathrm{C/cm^2}$ [8] and that of the highly c-axis oriented BLT is less than 30 $\mu\mathrm{C/cm^2}$ [9] at the same applied voltage. Other rare-earth-cations-modified capacitors also exhibited a highly c-axis oriented preferential growth and well-saturated *P-E* loops with large values of $2P_r$: 45–50 $\mu\mathrm{C/cm^2}$ for BPrT and BSmT, 80 $\mu\mathrm{C/cm^2}$ for BGdT.

The relative dielectric permittivity [$\varepsilon'(\omega)$] and the dissipation factor [$\tan\delta$] of the capacitor were 395 and 0.05, respectively, at a frequency of 1 MHz. These values are comparable to those of PZT, SBT, and BLT capacitors [8]. Although both $\varepsilon'(\omega)$ and $\tan\delta$ decreased slightly with increasing frequency, there was no sudden change in their values up to 1 MHz, suggesting that the observed *P-E* curve was originated from the ferroelectric polarization switching of bound charges.

We now examine the origin of large P_s observed in a series of BTs modified by rare-earth cations. For this purpose, the structural refinement was made by Rietveld analysis using synchrotron x-ray diffraction (XRD) patterns obtained from the 8C1 POSCO beam line of the Pohang Light Source (PLS). Figure 2 summarizes the structural refinement of the BNdT ($Bi_{4-x}Nd_xTi_3O_{12}$ with $x = 0.85$). The refined lattice parameters of the pseudotetragonal BNdT at 298 K are $a = 5.4055$ Å, $b = 5.4084$ Å, and $c = 32.8806$ Å. One important conclusion obtained from the refinement is that the major contribution to the development of P_s along the c axis (or z direction) comes from the TiO_6 octahedron unit adjacent to the interleaving Bi_2O_2 layer (Ti2 or Ti2′ site) rather than from the TiO_6 unit of the inner central octahedron layer (Ti1 site). The estimated off-center displacements of the central Ti ion at the Ti2 site with respect to the center of the six surrounding oxygen ions are 0.30 Å along the c axis and only 0.07 Å along the b axis [Fig. 2(c)]. This indicates that the polarization vector mainly develops along the c axis. Considering an asymmetric environment of the Ti2 site but a symmetric nature of the Ti1 site along the c axis, one does expect that the Ti2 site is the relevant site for developing giant P_s along the c axis [Figs. 2(b) and 2(c)]. The refined result thus suggests the existence of a highly

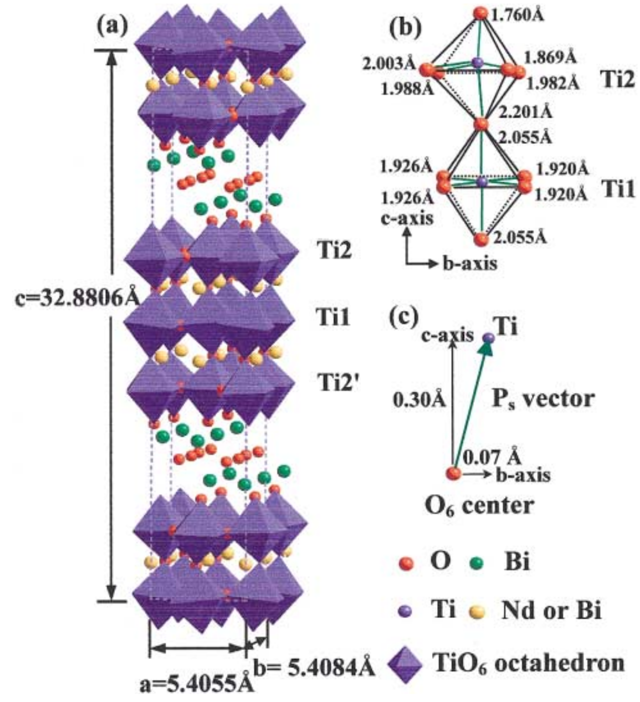

FIG. 2 (color). (a) The refined unit-cell structure of BNdT ($x = 0.85$) at 29 K. The Rietveld refinement was made using the DBWS program in the Cerius2 package. The degree of fitness in the refinement was quite satisfactory with $R_p = 4.42\%$ and $R_{\mathrm{wp}} = 6.68\%$. The refinement indicated that, within the three perovskite layers, the oxygen octahedra were canted each other both on the *a-b* plane and along the *c* axis with a zigzagging order, but the degree of canting into the *c*-axis direction of the octahedral layer decreased with increasing Nd modification. (b) The refined result of Ti1 and Ti2 sites projected on the *b-c* plane. Numerical values represent various real-space bond lengths between the central Ti ion and the surrounding oxygen ions. (c) The polarization vector of the Ti2 site projected on the *b-c* plane.

asymmetric double-well potential at the Ti2 site along the z direction.

Having established the Ti site responsible for the giant P_s along the c axis, we now examine some spectroscopic evidences that support or criticize the above conclusion. For this purpose, we have studied Ti-edge x-ray absorption using the 3C1 beam line of the PLS with the ring current of 150–107 mA at 2.5 GeV. Figure 3 shows the Ti K-edge XANES (x-ray absorption near-edge structure) spectra of the highly c-axis oriented BNdT film for both in-plane and out-of-plane directions with respect to the linear polarization vector. It is now known that the shoulder absorption at 4968 eV (A peak) is arising from the dipole-forbidden (but quadrupole-allowed) $1s \rightarrow 3d\,t_{2g}^1 e_g^0$ transition, while the peak at 4971 eV (B peak) is caused by the $1s \rightarrow 3d\,t_{2g}^0 e_g^1$ transition [14]. The peak intensities caused by these forbidden transitions increase with the degree of the local structural distortion [15,16] around the central Ti ion because the distortion leads to the $3d$-$4p$ orbital mixing that causes the dipole-allowed transition ($\Delta l = \pm 1$) due to a partial p character in the p-d hybridized orbital [15]. The observed higher intensity of the B peak, as compared to that of the A peak, reflects the fact that the $3d$-$4p$ orbital mixing is relatively stronger in the e_g orbital [14] because it has a strong directional character along the three principal axes (x, y, z) and thus participates in the σ bonding which is directly related to the off-center distortion.

As shown in Fig. 3, the XANES intensity of the B peak of the c-axis oriented BNdT film is substantially higher for the out-of-plane direction than the in-plane mode, indicating that the local structural distortion is greater along the c axis than the distortion parallel to the a-b plane. Thus, the XANES data support the conclusion deduced from the Rietveld refinement (Fig. 2). The inset (a) presents three XANES spectra simulated using the *ab initio* self-consistent-field (SCF) method [12]. The designation, "Ti1," for example, corresponds to the computed spectrum assuming that the K-edge spectrum is solely contributed from the distortion at the Ti1 site. The result supports the previous conclusion that the large off-center displacement and thus the observed giant P_s in the c-axis oriented film originates from the outer Ti2 site, not from the inner central Ti1 site.

As summarized in the inset (b) of Fig. 3, the substitution of lanthanides (Nd, Gd, Sm, Pr) for bismuth in BT partly reduced the oxidation state of Ti to trivalent, producing Ti ions with $3d^1$ electronic configuration [17]. This inevitably leads to the Jahn-Teller distortion. The Jahn-Teller theorem further suggests that a d^1 electron in an octahedral field occupies the d_{xy} orbital of the split t_{2g} and thus leads to the "z-in" distortion. The exact nature and its role in the development of giant P_s will be the subject of further investigation.

We now return to the technological side and examine the four important criteria for the realization of high-density NvFRAM: (i) *large sensing margin,* (ii) *fatigue-free property,* (iii) *no imprinting,* and (iv) *stable charge-retaining*

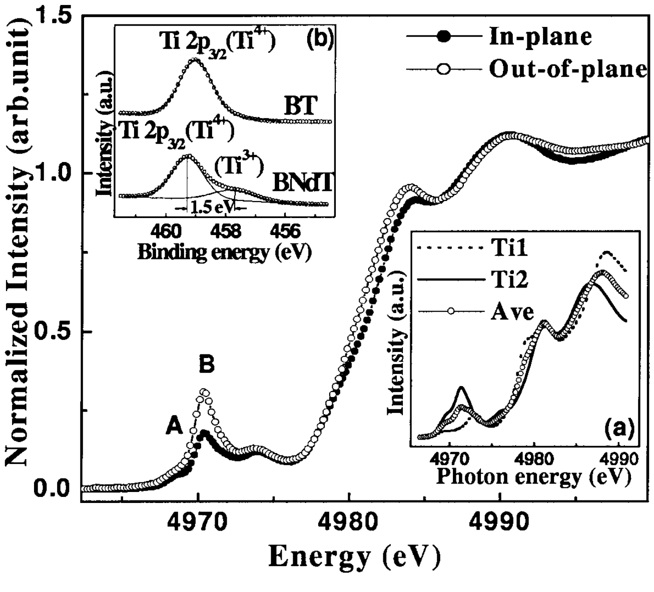

FIG. 3. Ti K-edge x-ray absorption spectra of the highly c-axis oriented BNdT film. The real-space SCF simulation [12] of XANES spectra presented in inset (a) was done using the FEFF8 module of the UWXAFS package [13]. The structural parameters refined by the Rietveld analysis were used as input parameters for the computation.

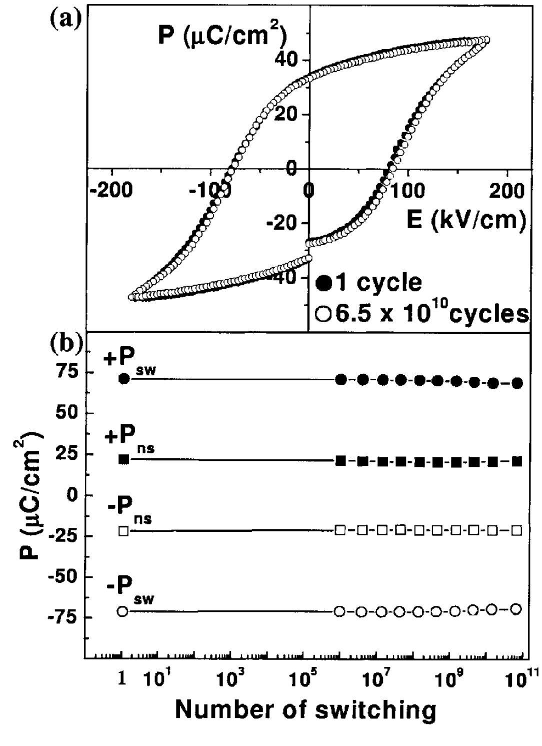

FIG. 4. Electrical fatigue characteristics of the Pt/BNdT/Pt capacitor. (a) P-E hysteresis loops measured at an applied voltage of 5 V before and after 6.5×10^{10} read/write switching cycles and (b) the fatigue-test results determined using a switching voltage of ± 3 V and a measuring voltage of 5 V at a frequency of 1 MHz.

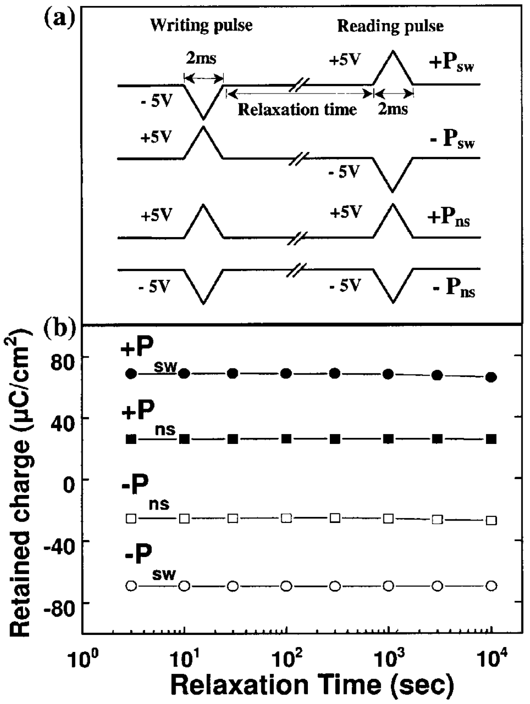

FIG. 5. Charge-retentions and imprinting characteristics of the Pt/BNdT/Pt capacitor at 85 °C. Panel (a) represents four distinctive test-pulse sequences employed.

ability. Figure 4 summarizes electrical fatigue characteristics of the Pt/BNdT/Pt capacitor. A typical area of the top electrode was 10^{-4} cm^2. As presented in Fig. 4, the capacitor shows little change in the switching polarization ($P_{\rm sw}$) and in the nonswitching polarization ($P_{\rm ns}$) up to 6.5×10^{10} switching cycles at a frequency of 1 MHz. The fatigue-free behavior was also observed at a higher switching voltage of ±5 V. The values of the nonvolatile charges [i.e., $(+P_{\rm sw}) - (+P_{\rm ns})$ or $(-P_{\rm sw}) - (-P_{\rm ns})$] measured at lower frequencies (between 1 kHz and 1 MHz) were also stable throughout the switching cycles. This type of fatigue-free behavior was observed in all four capacitors (BNdT, BGdT, BSmT, and BPrT) developed here. Another prominent feature of Fig. 4 is that the value of the nonvolatile charge is 54 μC/cm^2, and this value remains essentially constant throughout the switching cycles. The observed nonvolatile charge of 54 μC/cm^2 is by far the largest one among all known values for fatigue-free ferroelectric capacitors fabricated on conventional Pt electrodes. The values of $2P_r$ and E_c before the fatigue test were 67 μC/cm^2 and 77 kV/cm, respectively, at an applied voltage of 5 V. After being subjected to 6.5×10^{10} cycles, these were still retained at 66 μC/cm^2 and 78 kV/cm without any asymmetry in the *P-E* curve.

The charge-retention and imprinting characteristics of the BNdT capacitor are summarized in Fig. 5 by plotting the switching ($\pm P_{\rm sw}$) and the nonswitching polarization ($\pm P_{\rm ns}$) as a function of time at 85 °C. We measured the retained charges using the same capacitor and employing the following sequence: $+P_{\rm sw} \rightarrow -P_{\rm sw} \rightarrow +P_{\rm ns} \rightarrow -P_{\rm ns}$. As shown in Fig. 5, $|-P_{\rm sw}|$ is essentially the same as $+P_{\rm sw}$ throughout the relaxation time. The same trend was also observed for $|-P_{\rm ns}|$ and $+P_{\rm ns}$. This indicates that the capacitor has a strong resistance against the imprinting failure. The sensing margin for the identification of logical state, as defined by $P_{\rm nv} = (\pm P_{\rm sw}) - (\pm P_{\rm ns})$, was 45 μC/cm^2 and remained essentially constant up to 10^4 sec after applying a writing pulse, demonstrating a stable charge-retaining ability. Compared with the reported sensing margins [18] of *c*-axis oriented SBT capacitors (6 μC/cm^2) and of PZT capacitors (20 μC/cm^2), this is a remarkable improvement.

We have reported the development of a series of titanate-based layered perovskites having large values of the spontaneous polarization (P_s) with fatigue and imprinting-free characteristics. Among these, the BNdT/Pt system exhibited the most remarkable ferroelectric properties with its giant polarization along the *c* axis. Therefore, we would suggest reexamination of ferroelectric properties of Ti-based layered perovskites from a new standpoint.

This work was supported by the KISTEP of Korea through the NRL program.

---

*To whom correspondence should be addressed.
Email address: hmjang@postech.ac.kr

[1] J. F. Scott and C. A. Araujo, Science **246**, 1400 (1989).
[2] O. Auciello, J. F. Scott, and R. Ramesh, Phys. Today **51**, No. 7, 22 (1998).
[3] A. Kingon, Nature (London) **401**, 658 (1999).
[4] H. N. Al-Shareef, K. R. Bellur, A. I. Kingon, and O. Auciello, Appl. Phys. Lett. **66**, 239 (1995).
[5] K. B. Lee, S. Tirumala, and S. B. Desu, Appl. Phys. Lett. **74**, 1484 (1999).
[6] S. R. Shannigrahi and H. M. Jang, Appl. Phys. Lett. **79**, 1051 (2001).
[7] C. A. Araujo, J. D. Cuhairo, L. D. McMillan, M. C. Scott, and J. F. Scott, Nature (London) **374**, 627 (1995).
[8] B. H. Park *et al.*, Nature (London) **401**, 682 (1999).
[9] U. Chon, G.-C. Yi, and H. M. Jang, Appl. Phys. Lett. **78**, 658 (2001).
[10] U. Chon, H. M. Jang, S.-H. Lee, and G.-C. Yi, J. Mater. Res. **16**, 3124 (2001).
[11] R. W. Wolfe and R. E. Newnham, J. Electrochem. Soc. **116**, 832 (1969).
[12] A. L. Ankudinov, B. Ravel, J. J. Rehr, and S. D. Conradson, Phys. Rev. B **58**, 7565 (1998).
[13] A well-known *ab initio* simulation package for XAS, programmed by the J. J. Rehr group, University of Washington.
[14] R. V. Vedrinskii, V. L. Kraizman, A. A. Novakovich, Ph. V. Demekhin, and S. V. Urazhdin, J. Phys. Condens. Matter **10**, 9561 (1998).
[15] T. E. Westre *et al.*, J. Am. Chem. Soc. **119**, 6297 (1997).
[16] G. G. Li, F. Bridges, and C. H. Booth, Phys. Rev. B **52**, 6332 (1995).
[17] W. Göpel, Surf. Sci. **139**, 333 (1984).
[18] J. J. Lee, C. L. Thio, and S. B. Desu, Phys. Status Solidi (a) **151**, 171 (1995).